ISSN 0965-545X, Polymer Science, Series A, 2021, Vol. 63, No. 5, pp. 568–575. © Pleiades Publishing, Ltd., 2021.
ISSN 0965-545X, Polymer Science, Series A, 2021. © Pleiades Publishing, Ltd., 2021.

COMPOSITES

Polymer-Clay Nanocomposites: Exfoliation and Intercalation of Organophilic Montmorillonite Nanofillers in Styrene–Limonene Copolymer

Hodhaifa Derdar[a,b,*], Rachid Meghabar[b], Mohamed Benachour[b], Geoffrey Robert Mitchell[c], Khaldoun Bachari[a], Mohammed Belbachir[b], Zakaria Cherifi[a,b], Mohammed Chakib Baghdadli[b], and Amine Harrane[b,d]

[a] *Centre de Recherche Scientifique et Technique en Analyses Physico-Chimiques (CRAPC), BP 10 384, Siège ex-Pasna Zone Industrielle, Bou-Ismail CP 42004, Tipaza, Algeria*

[b] *Laboratoire de chimie des polymères. Département de chimie. Faculté des sciences exactes et appliquées. Université Oran1 Ahmed Benbella, BP 1524, El-Mnaouer, Oran, 31000 Algeria*

[c] *Centre for Rapid and Sustainable Product Development, Institute Polytechnic of Leiria, Marinha Grande, Portugal*

[d] *Department of Chemistry, FSEI University of Abdelhamid Ibn Badis–Mostaganem, Algeria*

** e-mail: hodhaifa-27@outlook.fr*

Received November 21, 2020; revised February 24, 2021; accepted April 3, 2021

Abstract—Nanocomposites from Styrene-Limonene copolymers and Algerian organophilic-clay named Maghnite-CTA$^+$ (Mag-CTA$^+$), were prepared by in-situ polymerization using different amounts (2, 5, and 10% by weight) of clay and Azobisisobutyronitrile (AIBN) as a catalyst. The Mag-CTA$^+$ is an organophilic silicate clay prepared through a direct exchange process, using Cetyltrimethylammonuim bromide (CTAB) in which it used as green nano-filler. The preparation method of nanocomposites was studied in order to determine and improve structural, morphological and thermal properties of Sty-Lim copolymer. The structure and morphology of the obtained nanocomposites (Sty-Lim/Mag) were determined using Fourier transform infrared spectroscopy (FTIR), X-ray diffraction (XRD), scanning electronic microscopy (SEM) and transmission electronic microscopy (TEM). The analyses confirmed the chemical modification of clay layers and the intercalation of Sty-Lim copolymer within the organophilic clay sheets. Exfoliated structure was obtained for the lower amount of clay (2 wt %), while intercalated structures were detected for higher amounts of clay (5 and 10 wt %). The thermal properties of the obtained nanocomposites were studied by thermogravimetric analysis (TGA) and show a significant improvement in the thermal stability compared with the pure copolymer. The obtained nanocomposites show an optimal degradation temperature of 320°C.

DOI: 10.1134/S0965545X21050023

INTRODUCTION

In the last decades, a growing interest is focused on a new class of materials, reinforced by nanoscale particles, called nanocomposites. Interest in these new materials was initiated by Toyota researchers in the early 1990s. In fact, by dispersing clays in polyamide-6 by in situ polymerization, they showed a significant increase in dimensional stability [1]. These results have been the precursor to new perspectives for polymer matrix nanocomposites in many scientific fields [2]. In recent years, nanocomposites based on toxic polymers have been replaced by others based on green materials. The use of a polymer matrix by adding a well-defined percentage of clay as reinforcement leads to the improvement of the physicochemical properties of the resulting nanocomposites such as high modulus, increased heat resistance, adhesion and barrier gas properties, flammability, and increased biodegradability of biodegradable polymers [3, 4]. Based on the interaction strength of the modified polymer/clay, two different types of nanocomposites structures can be synthesized, intercalated and exfoliated nanocomposites. The synthesis of nanocomposites can be done by different methods such as in situ polymerization, solution blending of polymer and other methods [5].

Styrene is one of the most studied and widely used monomers, whether in industry or in academic studies, because its polymerization is used as a model for chain polymerization [6] and it is used as a monomer to make plastics. Styrene is also used as a comonomer to produce copolymers with several other monomers, including acrylonitrile butadiene styrene (ABS) [7], rubber or latex based on styrene butadiene (SBS) [8], styrene-acrylonitrile (SAN) [9], acrylonitrile styrene acrylate (ASA) as well as unsaturated polyesters [10]. The production of styrene in particular increased very

quickly in the United States during the Second World War to meet the needs of synthetic rubber for the army. Styrene is also used in small amounts as an additive in perfumes or medicines [11] and in particular for the synthesis of polyester resins [12].

Limonene is a monocyclic terpene found in many essential oils extracted from citrus zest [13]. The first polymerization of terpenes was carried out in 1798, when Bishop Watson added a drop of sulfuric acid to produce a sticky resin [14]. Derdar et al. also studied the polymerization and the copolymerization of limonene using a green catalyst called Maghnite [15, 16]. The copolymerization of limonene with other monomers such as styrene was also attempted using azobisisobutyronitrile (AIBN) as a radical catalyst [17]. However, at that time, the researchers could not distinguish the interesting properties of this material, which further delayed its 50 yr study. In 1950, William Roberts studied the cationic polymerization of many terpenes such as limonene, α-pinene and β-pinene with Friedel-Crafts catalysts, for example $SnCl_4$ and $AlBr_3$ [18]. By adding less than 1% of catalyst in toluene, William Roberts produces a solid β-pinene polymer with a low molecular weight of about 1500 g/mol. The degree of polymerization of β-pinene, although very low, is higher than that of the two other monomers (limonene, α-pinene) [19, 20]. Limonene has been widely used in a wide range of products such as cosmetics, as food additives, medicine and even as a green solvent [21].

By examining the literature, we find that the use of natural clay as nano-reinforcing fillers in the synthesis of green-nanocomposites based on styrene-limonene copolymer and clay is practically nonexistent. The main goal of this work is to use an organo-modified montmorillonite clay named Mag-CTA^+ as a new nano-reinforcing filler in order to improve thermal properties of styrene-limonene copolymer, also, to prepare nanocomposites out of green raw materials (limonene and clay). In previously published work, we have shown the advantage of applying this type of nano-reinforcing fillers in several nanocomposites synthesis [22–24]. It is preferred for its many advantages such as a very low purchase price compared to other nano-reinforcing fillers.

EXPERIMENTAL

Materials and Methods

In this work we have used styrene (99%), (R)-(+)-limonene (97%), methanol (CH_3OH, 99.9%), toluene ($C_6H_5CH_3$, 99.8%), sodium chloride (NaCl), azobisisobutyronitrile (AIBN, 98%) and cetyltrimethylammonuim bromide (CTAB) were purchased by Sigma Aldrich and used as received. Maghnite (Algerian montmorillonite) is supplied in the raw state by ENOF Bental Spa of the National Company of Nonferrous Mining Products, Maghnia Unit (Algeria).

Preparation of the Maghnite-Na^+ (Mag-Na^+)

The Mag-Na^+ was prepared according to the process described in our previous study [25, 26]. 20 g of purified raw-Mag was mixed with 1 L of distilled water, then stirred during 2 h at 25°C, and left 8 h until the appearance of Montmorillonite supernatant. 10 mL of the supernatant were removed and mixed with 10 mL of distilled water, the mixture was stirred for 30 min, and again left stirring for 8 h. This operation was repeated until the complete recovery of Montmorillonite. The recovered Montmorillonite was filtered, dried, milled, and then brought into contact with a solution of NaCl (1 M) to exchange ions present in the clay by Na^+. It was then left stirring for 48 h, the Mag-Na^+ was then washed several times with distilled water to remove Cl^{-1} ions. At the end, Mag-Na^+ was filtered, dried in the oven at 105°C for 24 h, and it was then finely ground and stored in a dry place.

Preparation of the Organo-Clay (Mag-CTA^+)

Mag-CTA^+ is an organophilic clay exchanged with cetyltrimethylammonium (CTAB) cations from Mag-Na^+. The Mag-CTA^+ activation was carried out by ultrasound during 1 h [27]. Firstly 10 g of Mag-Na^+ was placed in a 1 L Erlenmeyer flask with the chosen concentration (1 CEC). At the end of the exchange process, the suspension was filtered and then washed several times with distilled water. Finally, the solid obtained was dried at 105°C during 24 h and then ground. The structure of organophylic clay was confirmed by FTIR and XRD analysis and their morphological properties were studied by SEM and TEM analysis.

Preparation of Nanocomposites (Sty-lim/Mag)

Sty-Lim/Mag nanocomposites were prepared using in situ polymerization method. 0.02 mol (2 g) of styrene and 0.02 mol (3 g) of limonene was dissolved in toluene, and then different amounts of organoclay (2, 5, and 10% by weight) were added to the mixture. The solution was then stirred for 5 min to completely dissolve the styrene and limonene in toluene. After that, the radical initiator Azobisisobutyronitrile (AIBN) was added to the mixture and stirred (500 rpm) under reflux at 90°C for 6 h (see Scheme 1). At the end of the reaction, the nanocomposite was recovered by precipitation in cold methanol, filtered and dried under vacuum overnight. The operating conditions are shown in Table 1.

Characterization

The functional groups of the modified clay and the obtained nanocomposites were analyzed by infrared spectroscopy FTIR in the range of 4000–360 cm^{-1} using BRUKER ALPHA Diamond-ATR. The surface

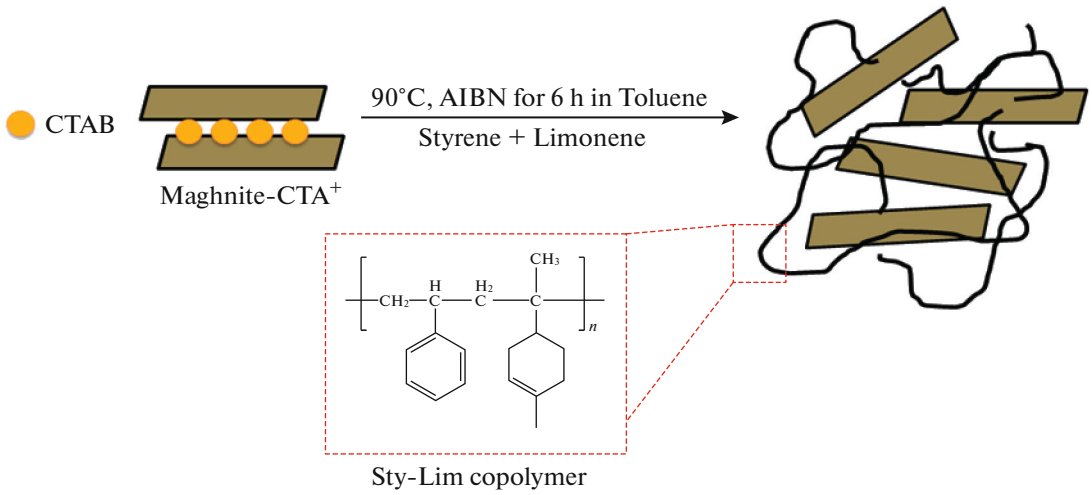

Scheme 1.

morphology of the modified clay and its nanocomposites were observed by XRD diffraction patterns using a Bruker AXS D8 diffractometer (CuK_α radiation), FEG-SEM on a, JEOL 7001F electron microscopy and Transmission electron micrographs were performed using a Hitachi 8100. Thermal properties were analyzed by thermogravimetric analysis (TGA) using a PerkinElmer STA 6000 under nitrogen in the temperature range of 30–700°C with a heating rate of 20 deg/min.

RESULTS AND DISCUSSION

Modified Clays (Mag-Na$^+$ and Mag-CTA$^+$)

The FTIR spectra of Mag-Na$^+$ and Mag-CTA$^+$ are shown in Fig. 1. The comparison between the two spectra FTIR corresponding to the Mag-Na$^+$ and the Mag-CTA$^+$ shows the functional modification in the organophilic montmorillonite and the intercalation of the alkylammonium ions in the galleries of the clay by exchange the ion Na$^+$ by cetyltrimethylammonium cations in Mag-Na$^+$. We observe an intense peak at 1057 cm^{-1} and two bands at 455 and 515 cm^{-1} relating to the elongation vibrations of the Si–O–Si and Si–O–Al bonds respectively [28, 29]. The band at 1000 cm^{-1} is due to the vibration of Si–O of the Maghnite. Different bands were obtained after the modification of Maghnite by CTA$^+$, two new bands were observed for Mag-CTA$^+$, in the 2850 and 2922 cm^{-1} regions corresponding to the C–H stretching vibrations of the methyl group. The results obtained by FTIR analysis confirm the intercalation of the alkyl ammonium ions of the CTAB between the clay sheets.

X-Ray diffractograms of Raw-Mag, Mag-Na$^+$ and Mag-CTA$^+$ are shown in Fig. 2. The calculated basal spacing (d_{001}) from XRD patterns, applying Bragg equation ($2d\sin\theta = n\lambda$) is 1.01 nm for Raw-Mag and 1.23 nm for Mag-H$^+$. This increase in basal spacing is explained by the atomic radius of Na$^+$ = 0.22 nm. The diffractograms of Mag-Na$^+$ and Mag-CTA$^+$ show that the interfoliar distance goes from d = 1.23 nm for the Mag-Na$^+$ which corresponds to the exchange by Na$^+$ in the galleries of Maghnite to d = 1.8 nm for the Mag-CTA$^+$. This increase indicates that there is intercalation of the alkyl ammonium ions of the CTAB in the inter-foliar galleries and a cationic exchange of Na$^+$ by CTA$^+$. The addition of the alkyl ammonium ions causes a displacement of the characteristic peak of the interfoliar distance of montmorillonite towards the weak nails (4.90 deg) for Mag-CTA$^+$. Aicha Khenifi et al. [30], obtained an interlayer distance of 1.98 nm during 24 h of stirring for the preparation of CTAB/Clay, in our case, an interlayer distance of 1.8 nm was obtained only in 1 h. Also, the X-ray pattern of the raw-Mag shows strong peaks of quartz and calcite at 2θ = 26°–29°. These peaks decrease in

Table 1. Experimental conditions for the preparation of Sty-Lim/Mag nanocomposites

Samples	Sty, g	Lim, g	Mag-CTA$^+$, wt %	Time, h	Yield, %
Sty-Lim/Mag 2%	2	3	2	6	86.3
Sty-Lim/Mag 5%	2	3	5	6	82.7
Sty-Lim/Mag 10%	2	3	10	6	79.6

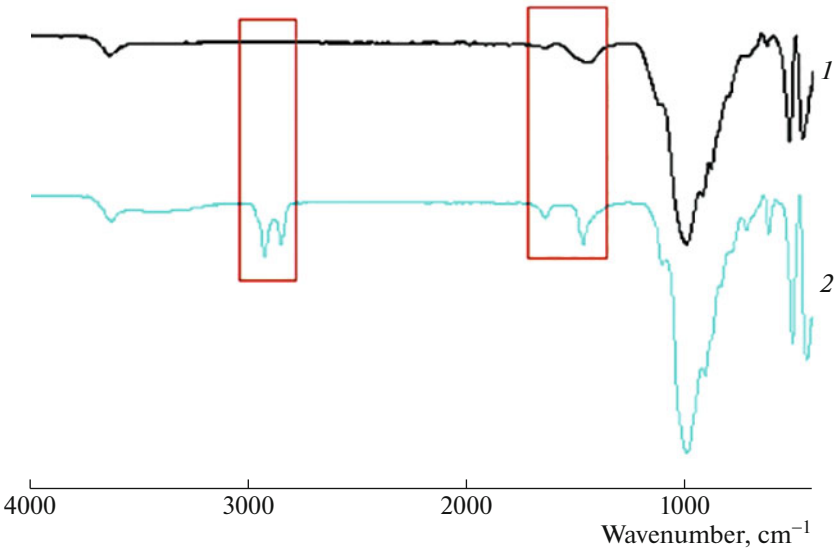

Fig. 1. FTIR spectra of (*1*) Mag-Na^+ and (*2*) Mag-CTA^+.

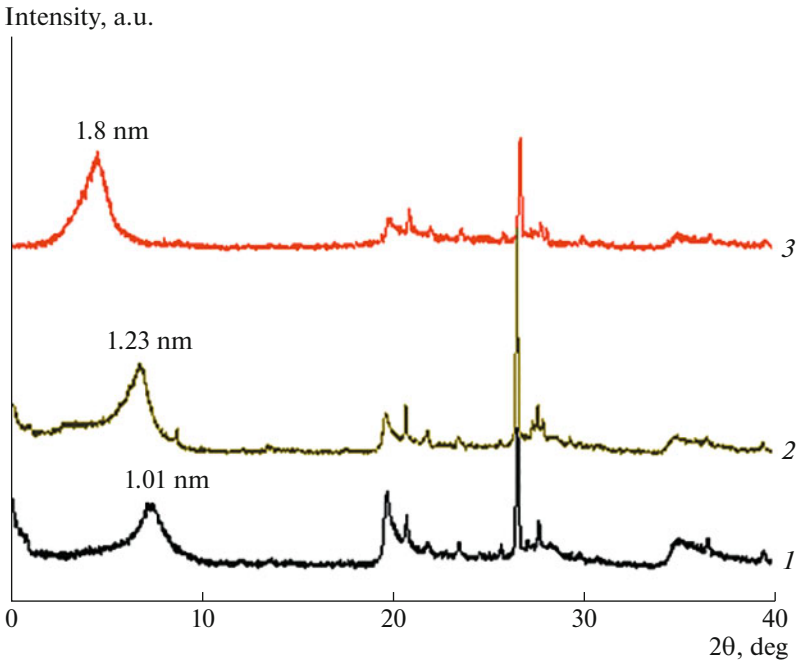

Fig. 2. XRD patterns of (*1*) Raw-Mag, (*2*) Mag-Na^+ and (*3*) Mag-CTA^+.

intensity in the diffractograms of Mag-Na^+ and Mag-CTA^+ thus indicating that the quantity of impurities was reduced after purification and modification of Maghnite. These results show the effect of ultrasonic irradiation on the preparation of Mag-CTA^+.

Obtained Nanocomposites (Sty-Lim/Mag)

The FTIR spectra of the obtained nanocomposites (Sty-Lim/Mag 2, 5 and 10%) and pure copolymer (Sty-Lim) are shown in Fig. 3. The infrared spectra show that the copolymer and the nanocomposites have almost the same vibration bands overlapping with the vibration bands of the organo-modified clay (Mag-CTA^+) and the FTIR spectra show that the obtained nanocomposites Sty-Lim/Mag are in a good agreement with the copolymer structure. The adsorption band at 695 cm^{-1} corresponds to the vibration of the benzyl cycle in styrene and the adsorption band at 1673 cm^{-1} corresponds to the double bond C=C in the polylimonene were observed in the FTIR spectra of the obtained nanocomposites. The C–H symmetric

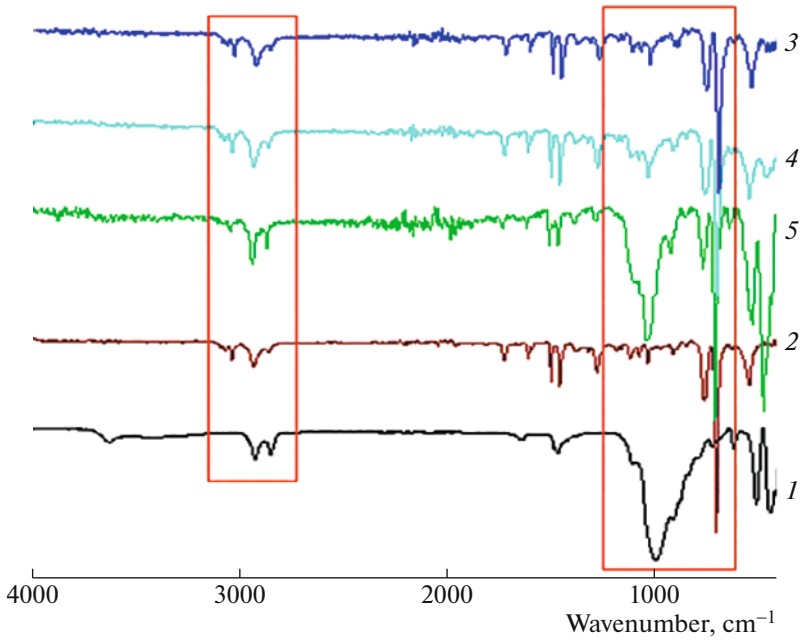

Fig. 3. FTIR spectra of (*1*) Mag-CTA$^+$, (*2*) Sty-Lim and the obtained nanocomposites Sty-Lim/Mag: (*3*) 2, (*4*) 5 and (*5*) 10%.

and asymmetric stretching of the methyl and methylene group was observed at 2922 and 2935 cm^{-1}. Compared with the FTIR spectrum of the pure copolymer, the spectra of the obtained nanocomposites show the appearance of the intense peak at 1000 cm^{-1} corresponding to the vibration of Si–O of the Mag-CTA$^+$. However, the absorption bands observed on the FTIR spectra of Sty-Lim and Mag-CTA$^+$ are gathered on the FTIR spectra of the obtained nanocomposites. These results confirm the interaction of the functional group of the copolymer with the internal surface of clay.

The XRD patterns of the obtained nanocomposites and the pure copolymer are shown in Fig. 4. The XRD pattern of Sty-Lim copolymer presents no sharp peak confirming its amorphous structure. This amorphous structure is observed in the XRD patterns of the nanocomposites with the appearance of additional peak characteristic of Mag-CTA$^+$ which confirms its good dispersion in the copolymer matrix. The nanocomposites prepared by 5 and 10% by weight of Mag-CTA$^+$ showed a single peak around $2\theta = 2°$ and 2.5° corresponding to the interlayer distances $d_{001} = 4.01$ and 3.02 nm respectively. The interlayer distance of these nanocomposites was increased more than twice compared to the Mag-CTA$^+$, which had an interlayer distance of 1.8 nm. This result also confirms that the copolymer was well intercalated between the clay galleries. Except for the case of the nanocomposites obtained by 2% by weight of Mag-CTA$^+$, the diffraction peak of Mag-CTA$^+$ was not observed, confirming the exfoliation of the clay, which explains a good diffusion of the Sty-Lim copolymer in the clay galleries. These results are in agreement with those obtained by Hanène Salmi-Mani et al. [31].

Figure 5 shows the SEM images of the organo-modified clay (Mag-CTA$^+$), the intercalated nanocomposites (Sty-Lim/Mag 5 and 10%) and the exfoliated nanocomposites (Sty-Lim/Mag 2%). The comparison of the Mag-CTA$^+$ morphology (Fig. 5a) with the intercalated nanocomposites Sty-Lim/Mag 10 and 5% (Fig. 5b) at 5 μm shows a more organized small particle structure of montmorillonite, the same observation about the nanocomposites Sty-Lim/Mag 5% at 10 and 5 μm. In the nanocomposites Sty-Lim/Mag 2% (Fig. 5d), the observation of nanocomposites at 5 μm reveals a formation of montmorillonite plate separated and shows a rougher surface and a covering of the montmorillonite surface by the copolymer, that is a total or partial exfoliation.

The transmission electron microscopy was used to determine the dispersion of Mag-CTA$^+$ in Sty-Lim copolymer matrix and also to confirm the results obtained by the XRD analysis. The TEM images of Mag-CTA$^+$ and the obtained nanocomposites Sty-Lim/Mag (2, 5 and 10%) are shown in Fig. 6. For Mag-CTA$^+$ (Fig. 6a), it is easy to define the silicate layers by the dark and bright lines. The nanocomposites (Sty-Lim/Mag 10 and 5%) show an intercalated structure of the modified clay. However, the nanocomposite (Sty-Lim/Mag 2%) shows a partial or total exfoliated structure and the clay nanoparticles are mainly well dispersed in the copolymer matrix. These results confirm the results obtained by XRD analysis.

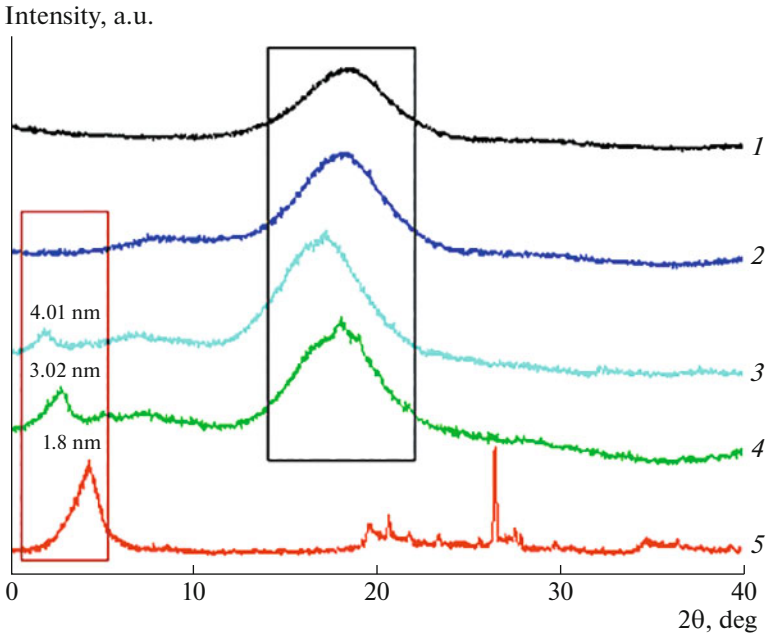

Fig. 4. XRD patterns of (*1*) Sty-Lim, nanocomposites Sty-Lim/Mag: (*2*) 2, (*3*) 5 and (*4*) 10%, and (*5*) Mag-CTA$^+$.

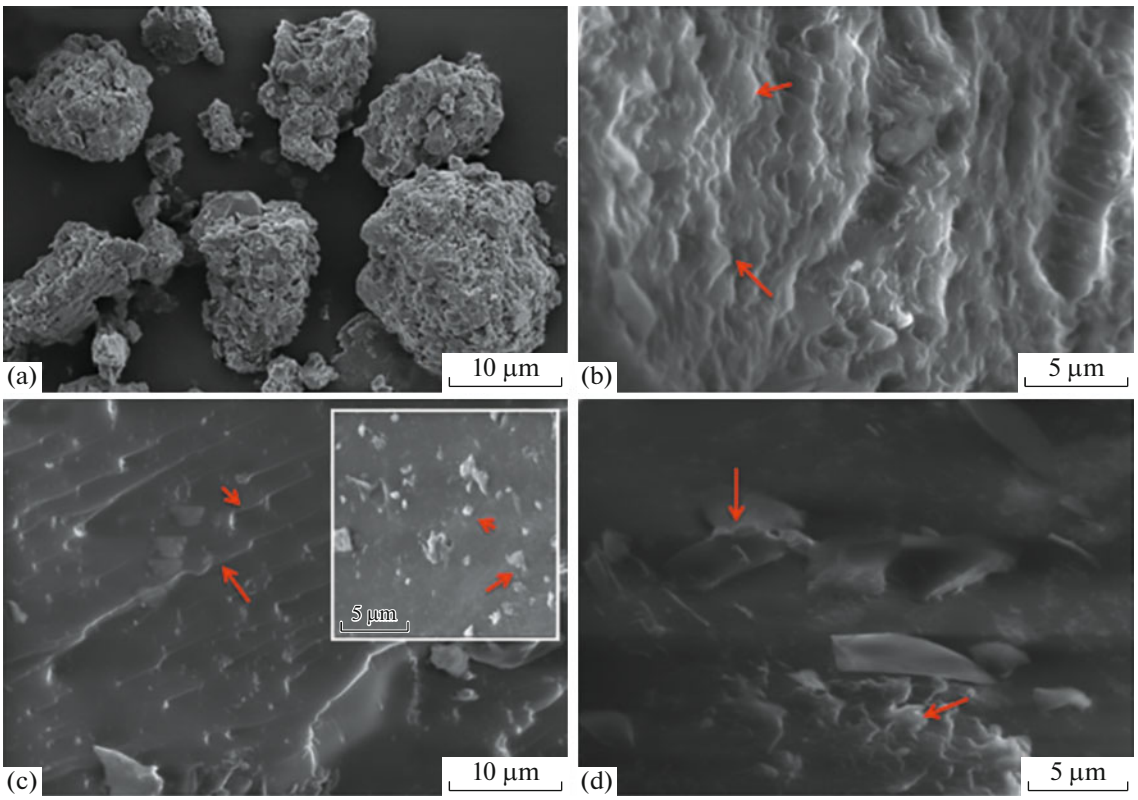

Fig. 5. SEM images of (a) Mag-CTA$^+$, (b) Sty-Lim/Mag 10%, (c) Sty-Lim/Mag 5% and (d) Sty-Lim/Mag 2%.

Thermogravimetric analysis was carried out under nitrogen with a heating rate of 20 grad/min. Figure 7 shows the TGA curves of pure copolymer and that of nanocomposites of 2, 5 and 10% by weight of Mag-CTA$^+$. It can be seen that the pure copolymer and all its nanocomposites exhibit a one-step weight loss mechanism. The nanocomposites show a higher thermal stability up to a degradation temperature of 270°C

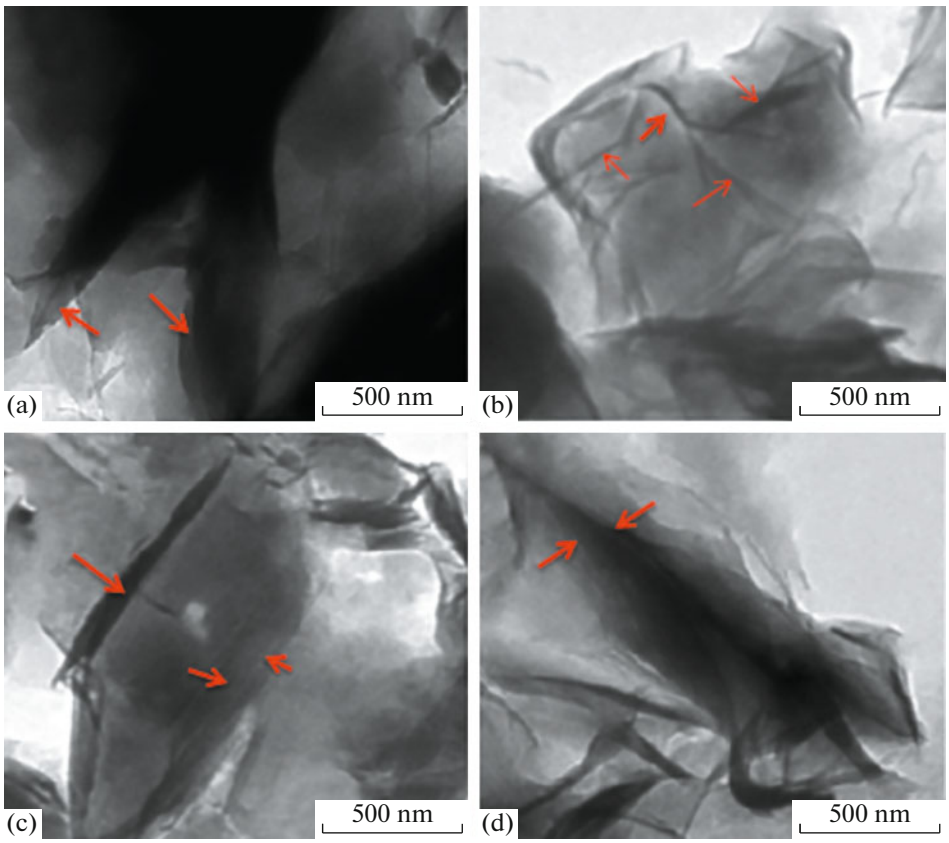

Fig. 6. TEM images of (a) Mag-CTA$^+$, (b) Sty-Lim/Mag-CTA 2%, (c) Sty-Lim/Mag-CTA 5%, (d) Sty-Lim/Mag-CTA 10%.

for the nanocomposite Sty-Lim/Mag 2%, while the degradation temperature of pure copolymer observed about 230°C. In addition, the intercalated nanocomposites Sty-Lim/Mag 10% showed a highest thermal stability with a degradation temperature of 320°C. These results show that the thermal stability of the obtained nanocomposites is not only related to the clay content but it is also much more linked to the state of the clay in the polymeric matrix and to the surface area between the polymeric matrix and the clay. This gain in thermal stability is due, according to previous work [32], to the formation of a protective carbonized layer. The formation of this layer is favored by the fine dispersion of intercalated or exfoliated particles of montmorillonite which play an inorganic support role [33]. In general, the degradation temperature of the polymers is increased after the incorporation of exfoliated lamellar silicates [34–36], which values these polymers and allows their use at higher temperatures.

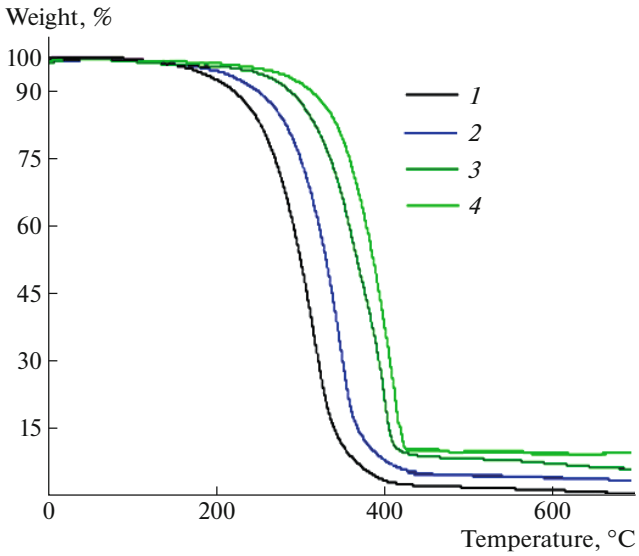

Fig. 7. TGA curves of (*1*) Sty-Lim copolymer and Sty-Lim/Mag nanocomposites: (*2*) 2, (*3*) 5, and (*4*) 10%.

CONCLUSIONS

The study shows that the different ratios of the organoclay (Mag-CTA$^+$) has an impact in the preparation of nanocomposites Styrene-Limonene copolymer. The XRD results indicate that the nanocomposite prepared with 2 wt % of Mag-CTA$^+$ was exfoliated, and the nanocomposites prepared with 5 and 10 wt % of Mag-CTA$^+$ were intercalated, leading to an expansion of the interlayer distance between the layers. Thermogravimetric results indicate that the nano-

composites present a higher thermal stability compared with the pure copolymer ($T < 320$°C). This is attributed to the interactions between all the copolymer chains and the organic compounds of the modified clay. The reinforcing effect of the clay in the copolymer is confirmed by increasing the degradation temperature of the system. The morphology study by SEM and TEM of the obtained nanocomposites confirmed an organization of certain particles, and in other cases a separation in plates made up of montmorillonite layers, this confirms partial or total exfoliation of montmorillonite in the copolymer matrix and formation of the nanocomposites.

CONFLICT OF INTEREST

The authors declare that they have no conflict of interest.

ACKNOWLEDGMENTS

We would like to thank the (DGRSDT) Direction Générale de la Recherche Scientifique et du Développement Technologique-Algeria, and the CDRSP-IPLeiria (Centre For Rapid and Sustainable Product Development) for giving us access to their STA device. We also would like to thank Dr A. Zaoui for help and advice through all the writing process.

REFERENCES

1. Y. Kojima, A. Usuki, M. Kawasumi, A. Okada, Y. F. Ukushima, and O. Kamigaito, J. Mater. Res. **8**, 1185 (1993).
2. A. Harrane, R. Meghabar, and M. Belbachir, Des. Monomers Polym. **9**, 181 (2006).
3. Y. Zare, M. Fasihi, and K. Y. Rhee, Appl. Clay Sci. **143**, 265 (2017).
4. M. Kotal and A. K. Bhowmick, Prog. Polym. Sci. **51**, 127 (2015)
5. M. Suslin, O. Nedilko, and D. Mishurov, Int. Biodeterior. Biodegrad. **110**, 136 (2016).
6. E. Yousif and R. Haddad, SpringerPlus **2**, 398 (2013).
7. B. Lai, Y. Zhou, H. Qin, C. Wu, C. Pang, Y. Lian, and J. Xu, Chem. Eng. J. **179**, 1 (2012).
8. J. Zhang, H. Chen, and Y. Zhou, Polym. Bull. **70**, 2829 (2013).
9. R. R. Devi and T. K. Maji, Wood Sci. Technol. **46**, 299 (2012).
10. Z. Mao and J. Zhang, Appl. Surf. Sci. **444**, 345 (2018),
11. K. Huang, S. Yu, and X. Li, J. Chem. Sci. **132**, 139 (2020).
12. M. S. Lima, C. S. M. F. Costa, J. F. J. Coelho, A. C. Fonseca, and A. C. Serra, Green Chem. **20**, 4880 (2018).
13. J. Sun, Altern. Med. Rev. **12**, 259 (2007).
14. E. Rukel, R. Wojcik, and H. Arlt, J. Macromol. Sci., Chem. **10**, 1371 (1976).
15. H. Derdar, M. Belbachir, and A. Harrane, Bull. Chem. React. Eng. Catal. **14**, 69 (2019).
16. H. Derdar, M. Belbachir, F. Hennaoui, M. Akeb, and A. Harrane, Polym. Sci., Ser. B **60**, 555 (2018).
17. S. Sharma and A. K. Srivastava, Eur. Polym. J. **40**, 2235 (2004).
18. W. Roberts and A. Day, J. Am. Chem. Soc. **72**, 1226 (1950).
19. M. Modena, R. B. Bates, and S. C. Marvel, J. Polym. Sci., Part. A: Gen. Pap. **3**, 949 (1965).
20. M. T. Barros, K. T. Petrova, and A. M. Ramos, Eur. J. Org. Chem. **8**, 1357 (2007).
21. R. T. Mathers and K. Damodaran, J. Polym. Sci., Part A: Polym. Chem. **45**, 3150 (2007).
22. H. Derdar, G. R. Mitchell, V. S. Mahendra, M. Benachour, S. Haoue, Z. Cherifi, K. Bachari, A. Harrane, and R. Meghabar, Polymers **12**, 1971 (2020).
23. N. Embarek, N. Sahli, and M. Belbachir, J. Compos. Mater. **53**, 4313 (2019).
24. Z. Cherifi, B. Boukoussa, A. Zaoui, M. Belbachir, and R. Meghabar, Ultrason. Sonochem. **48**, 188 (2018).
25. N. Embarek and N. Sahli, Bull. Chem. React. Eng. Catal. **15**, 290 (2020).
26. S. Haoue, H. Derdar, M. Belbachir, and A. Harrane, Bull. Chem. React. Eng. Catal. **15**, 221 (2020).
27. H. Derdar, G. R. Mitchell, Z. Cherifi, M. Belbachir, M. Benachour, R. Meghabar, K. Bachari, and A. Harrane, Bull. Chem. React. Eng. Catal. **15**, 798 (2020).
28. B. Cicel, Geol. Carpathica Ser. Clays **43**, 3 (1992).
29. A. Grenier and H. Wendorff, Angew. Chem., Int. Ed. **46**, 5670 (2007).
30. A. Khenifi, B. Zohra, B. Kahina, H. Houari, and D. Zoubir, Chem. Eng. J. **146**, 345 (2009).
31. H. Salmi-Mani, Z. Ait-Touchente, A. Lamouri, B. Carbonnier, J. F. Caron, K. Benzarti, and M. M. Chehimi, RSC Adv. **6**, 88126 (2016).
32. M. N. Bureau, J. Denault, K. C. Cole, and G. D. Enright, Polym. Eng. Sci. **42**, 1897 (2002).
33. D. E. Kherroub, M. Belbachir, and S. Lamouri, Res. Chem. Int. **41**, 5217 (2014).
34. R. A. Vaia, G. Price, P. N. Ruth, H. T. Nguyen, and J. Lichtenhan, Appl. Clay Sci. **15**, 67 (1999).
35. Z. K. Zhu, Y. Yang, J. Yin, X. Y. Wang, Y. C. Ke, and Z. N. Qi, J. Appl. Polym. Sci. **73**, 2063 (1999).
36. S. Wang, C. Long, X. Wang, Q. Li, and Z. Qi, J. Appl. Polym. Sci. **69**, 1557 (1998).